eLIFE
elifesciences.org

RESEARCH ARTICLE

Figures and figure supplements

VEGF-C promotes the development of lymphatics in bone and bone loss

Devon Hominick *et al*

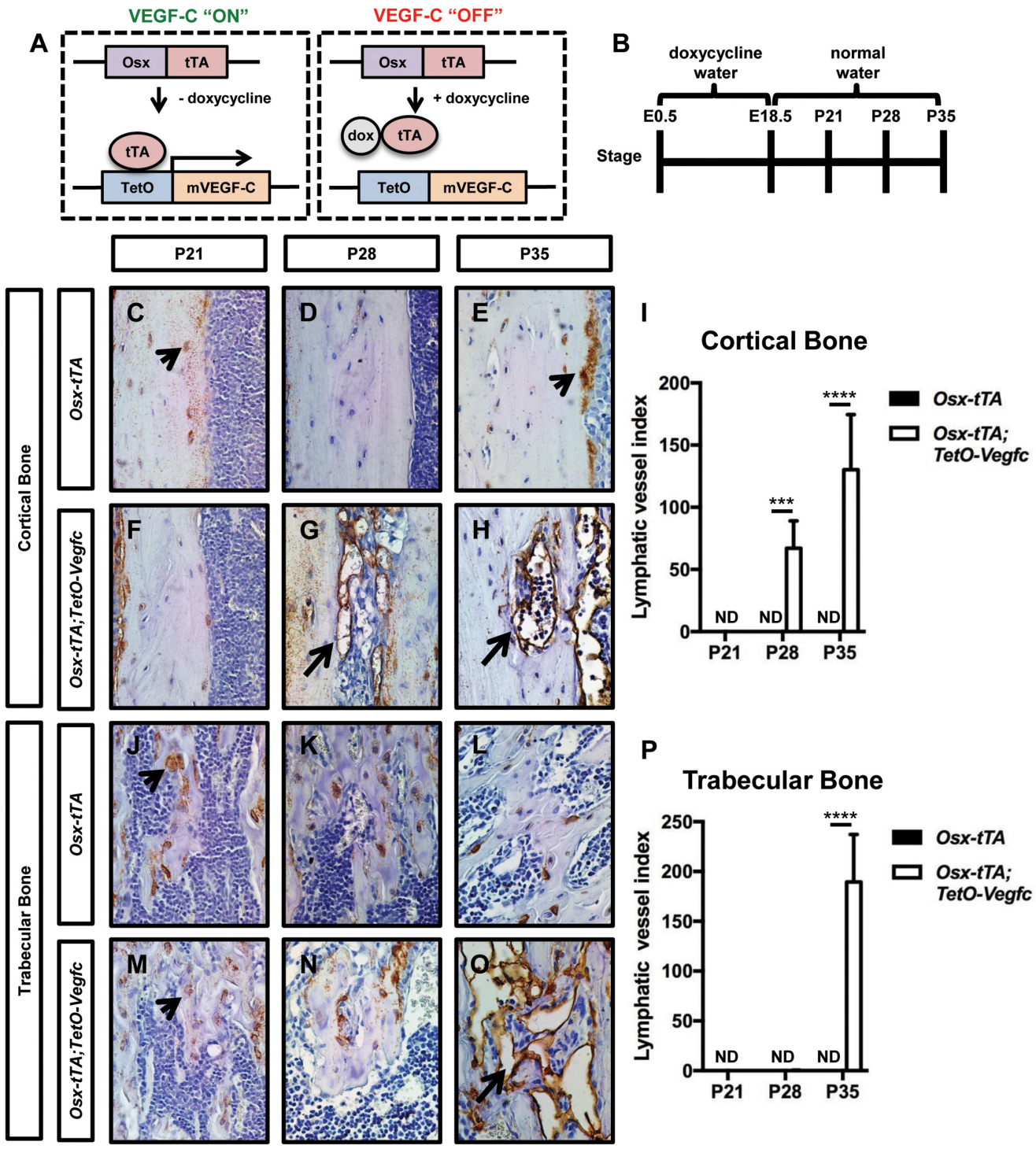

Figure 1. *Osx-tTA;TetO-Vegfc* mice develop lymphatics in their bones. (**A**) Schematic of the Tet-Off system used to express VEGF-C in bone. Doxycycline inhibits the expression of VEGF-C. (**B**) Schematic showing when mice received normal water and doxycycline water. *Osx-tTA* and *Osx-tTA; TetO-Vegfc* mice received doxycycline water from E0.5 to E18.5 and then normal water from E18.5 to P35. (**C–H**) Representative images of cortical bone

Figure 1 continued on next page

Figure 1 continued

in *Osx-tTA* and *Osx-tTA;TetO-Vegfc* femurs. Sections were stained with an anti-podoplanin antibody. Arrowheads point to podoplanin-positive osteocytes. Arrows point to podoplanin-positive lymphatics. (**I**) Graph showing lymphatic vessel index values for cortical bone in P21 (0 ± 0.0; n = 3), P28 (0 ± 0.0; n = 5), and P35 (0 ± 0.0; n = 6) *Osx-tTA* mice and in P21 (0 ± 0.0; n = 4), P28 (67 ± 22.06; n = 4), and P35 (130.3 ± 44.35; n = 4) *Osx-tTA;TetO-Vegfc* mice. (**J–O**) Representative images of trabecular bone in *Osx-tTA* and *Osx-tTA;TetO-Vegfc* femurs. Sections were stained with an anti-podoplanin antibody. Arrowheads point to podoplanin-positive osteocytes. Arrow points to podoplanin-positive lymphatics. (**P**) Graph showing lymphatic vessel index values for trabecular bone in P21 (0 ± 0.0; n = 3), P28 (0 ± 0.0; n = 5), and P35 (0 ± 0.0; n = 6) *Osx-tTA* mice and P21 (0 ± 0.0; n = 4), P28 (0.167 ± 0.4082; n = 6), and P35 (189.5 ± 47.7; n = 4) *Osx-tTA;TetO-Vegfc* mice. (***p<0.001, ****p<0.0001, unpaired student's T-test). ND = Not Detected.

DOI: https://doi.org/10.7554/eLife.34323.002

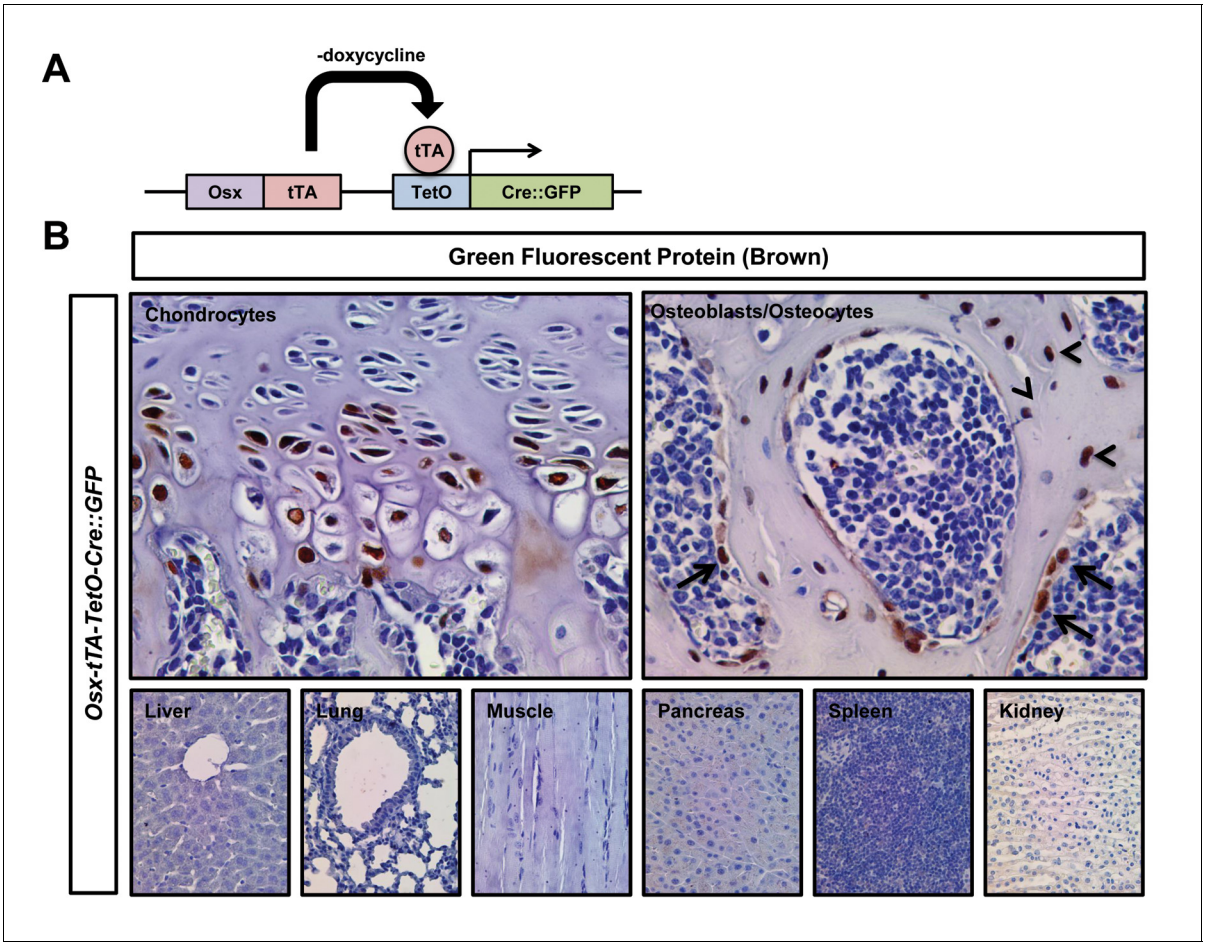

Figure 1—figure supplement 1. Expression pattern of GFP in *Osx-tTA-TetO-tTA-Cre::GFP* mice. (**A**) Schematic of the *Osx-tTA-TetO-tTA-Cre::GFP* cassette. When doxycycline is absent, tetracycline transactivator (tTA) induces the expression of a Cre::GFP fusion protein. (**B**) Representative images of tissues stained with an anti-GFP antibody. Tissues were collected from P35 *Osx-tTA-TetO-tTA-Cre::GFP* mice that were maintained on normal water. Chondrocytes, osteocytes (arrowheads), and osteoblasts (arrows) expressed GFP. Cells in the liver, lung, muscle, pancreas, spleen, and kidney did not express GFP.

DOI: https://doi.org/10.7554/eLife.34323.003

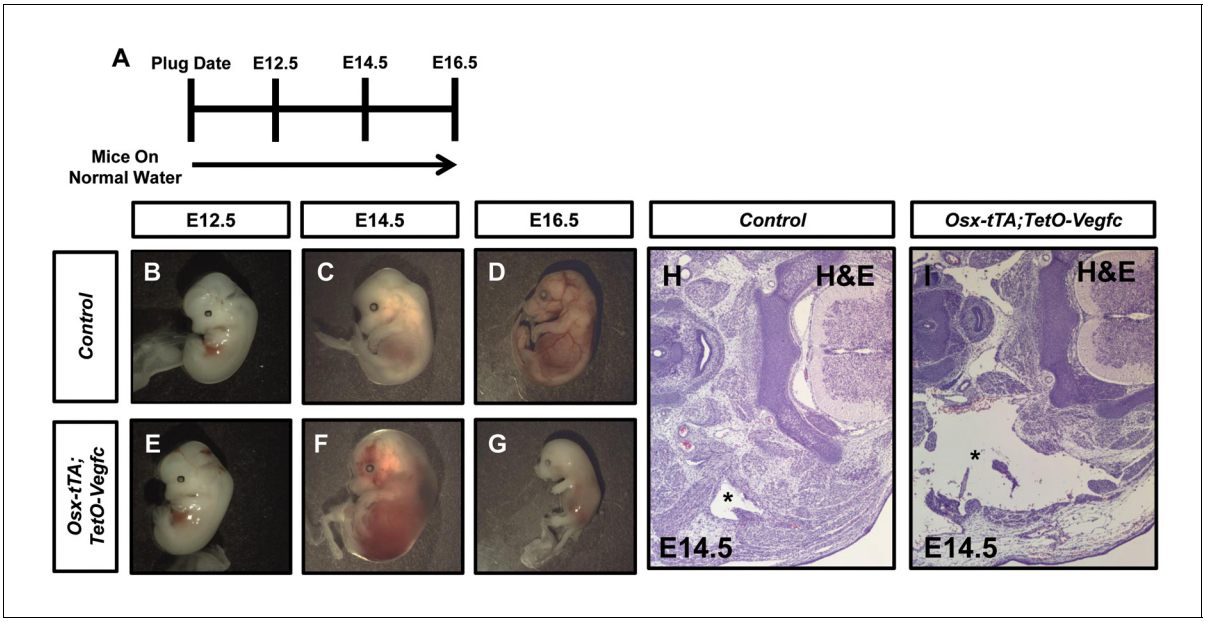

Figure 1—figure supplement 2. Expression of VEGF-C during embryonic development causes embryonic lethality. (**A**) Schematic showing when mice received normal water. (**B–C**) Representative images of E12.5, E14.5 and E16.5 control embryos. (**E–G**) Representative images of E12.5, E14.5 and E16.5 *Osx-tTA;TetO-Vegfc* embryos. (**H,I**) Transverse sections of E14.5 embryos stained with hematoxylin and eosin. The jugular lymph sac (asterisk) in the control embryo appears normal. In contrast, the jugular lymph sac (asterisk) in the *Osx-tTA;TetO-Vegfc* embryo is enlarged.

DOI: https://doi.org/10.7554/eLife.34323.004

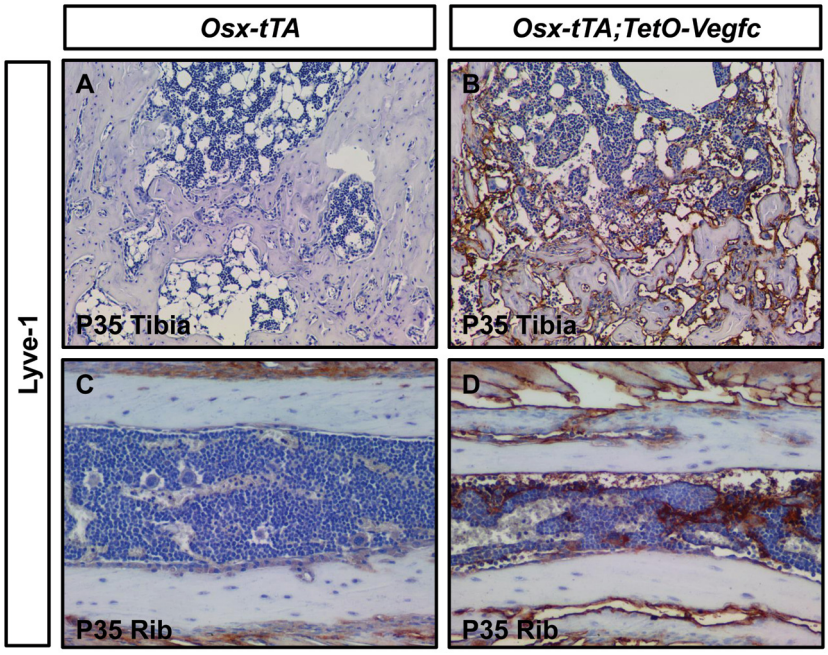

Figure 1—figure supplement 3. Bone lymphatics express Lyve-1. (**A**) No Lyve-1-positive cells are in tibias from P35 *Osx-tTA* mice. (**B**) Numerous Lyve-1-positive lymphatics are in tibias from P35 *Osx-tTA;TetO-Vegfc* mice. (**C**) No Lyve-1-positive cells are in ribs from P35 *Osx-tTA* mice. (**D**) Numerous Lyve-1-positive lymphatics are in ribs from P35 *Osx-tTA;TetO-Vegfc* mice.

DOI: https://doi.org/10.7554/eLife.34323.005

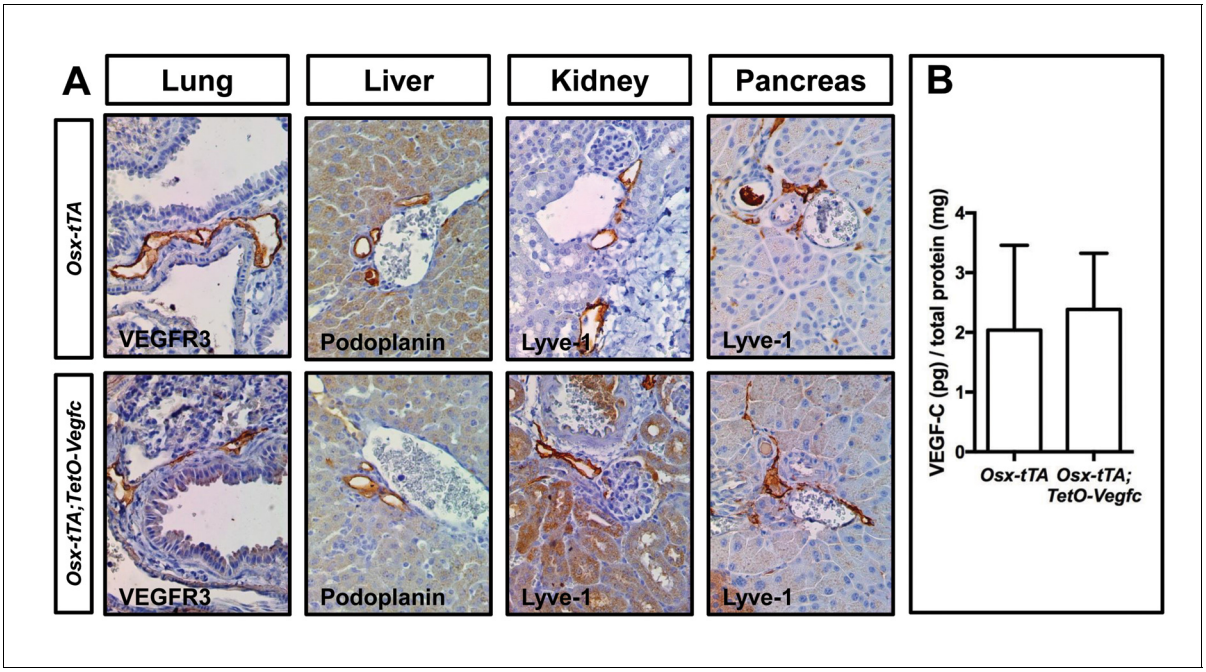

Figure 1—figure supplement 4. Lymphatics in soft tissues in *Osx-tTA;TetO-Vegfc* mice appear normal. (**A**) Representative pictures of tissues collected from P35 *Osx-tTA* and *Osx-tTA;TetO-Vegfc* mice. Lymphatics in the lung, liver, kidney, and pancreas appeared normal in *Osx-tTA;TetO-Vegfc* mice. (**B**) Graph showing the circulating level of VEGF-C in P35 *Osx-tTA* (2.04 ± 1.42, n = 8) and *Osx-tTA;TetO-Vegfc* (2.387 ± 0.94, n = 7) mice.

DOI: https://doi.org/10.7554/eLife.34323.006

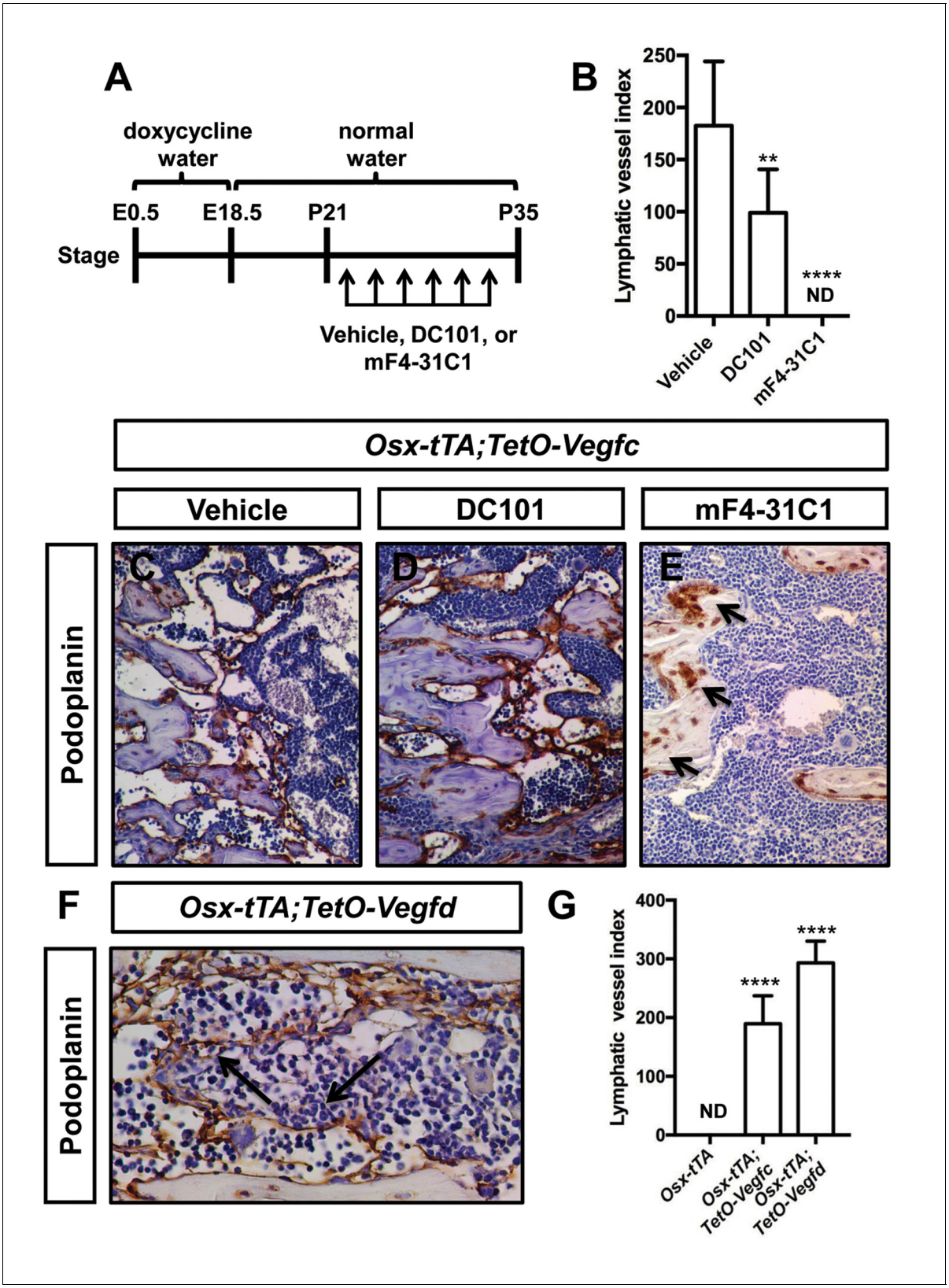

Figure 2. VEGFR3 signaling promotes the formation of bone lymphatics. (**A**) Schematic showing when mice received normal water and doxycycline water. *Osx-tTA;TetO-Vegfc* mice were treated (3x/week) with vehicle, DC101 (VEGFR2 function-blocking antibody), or mF4-31C1 (VEGFR3 function-blocking antibody) from P21 to P35. (**B**) Graph showing lymphatic index values for vehicle-treated (182.6 ± 61.56; n = 7), DC101-treated (99 ± 41.68;

Figure 2 continued on next page

Figure 2 continued

n = 7), and mF4-31C1-treated mice (0 ± 0.0; n = 5). (**p<0.01, ****p<0.0001, ANOVA followed by Dunnett's multiple comparisons test. Values were tested against values for vehicle-treated mice). (**C–E**) Representative images of femurs stained with an anti-podoplanin antibody. The femurs are from P35 mice. Arrows in panel E point to podoplanin-positive osteocytes. (**F**) Representative image of a femur from an *Osx-tTA;TetO-Vegfd* mouse that was stained with an anti-podoplanin antibody. Arrows point to podoplanin-positive lymphatics in the bone marrow. (**G**) Graph showing lymphatic vessel index values for trabecular bone in P35 *Osx-tTA* mice (0 ± 0; n = 6), *Osx-tTA;TetO-Vegfc* mice (189.5 ± 47.7; n = 4), and *Osx-tTA;TetO-Vegfd* mice (293 ± 37.24; n = 3). (****p<0.0001, ANOVA followed by Dunnett's multiple comparisons test. Values were tested against values for *Osx-tTA* mice). ND = Not Detected.

DOI: https://doi.org/10.7554/eLife.34323.007

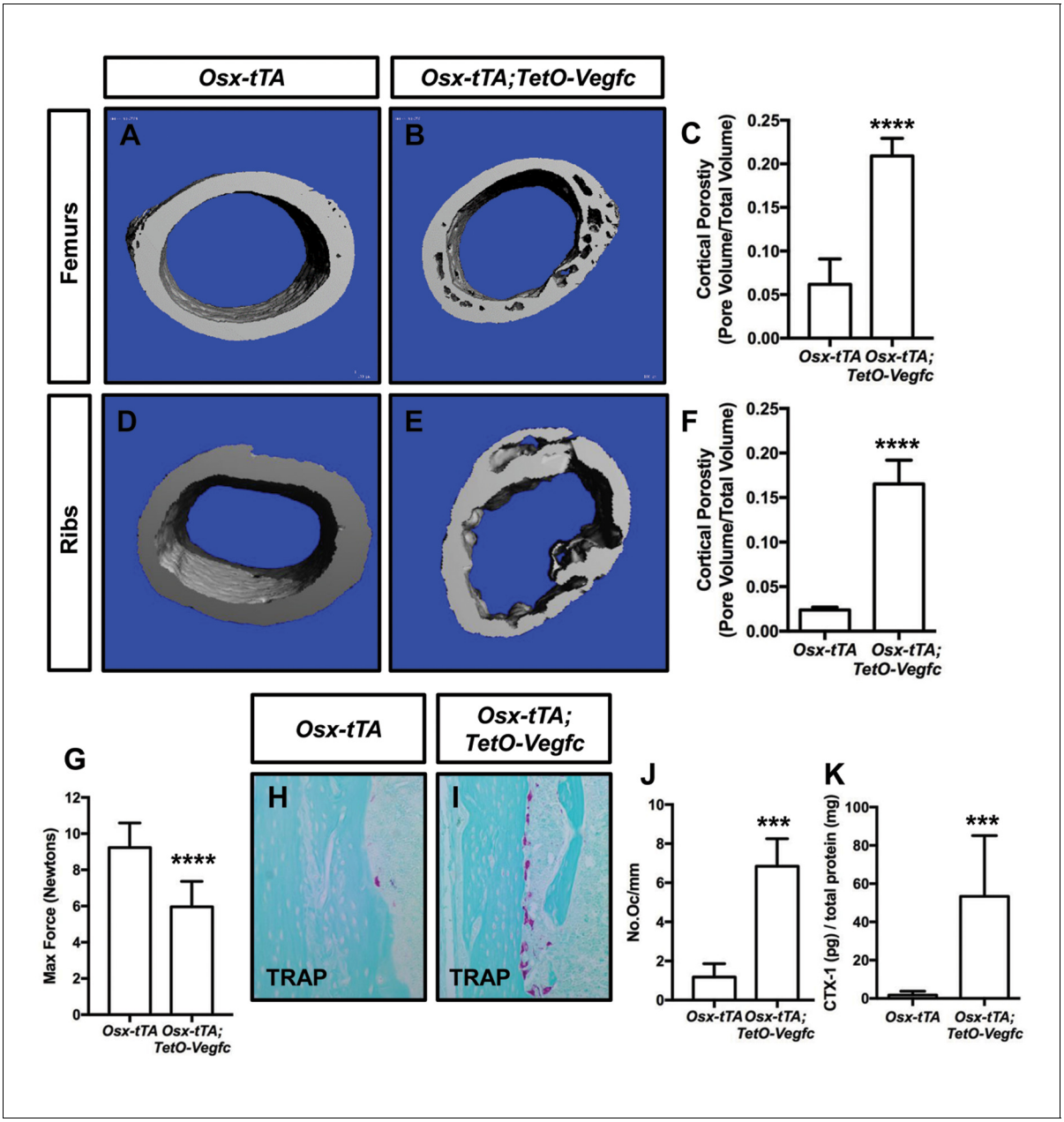

Figure 3. *Osx-tTA;TetO-Vegfc* mice have more porous bones and osteoclasts than *Osx-tTA* mice. (**A,B**) Representative µCT images of femurs from *Osx-tTA* and *Osx-tTA;TetO-Vegfc mice*. (**C**) Graph showing cortical bone porosity for femurs from *Osx-TA* (0.062 ± 0.0292, n = 5) and *Osx-tTA;TetO-Vegfc* (0.209 ± 0.0204, n = 6) mice. (**D,E**) Representative µCT images of ribs from *Osx-tTA* and *Osx-tTA;TetO-Vegfc mice*. (**F**) Graph showing cortical bone porosity for ribs from *Osx-TA* (0.024 ± 0.00293, n = 4) and *Osx-tTA;TetO-Vegfc* (0.165 ± 0.0265, n = 4) mice. (**G**) Graph showing results from the three-point bending assay. Less force was required to break bones from *Osx-TA;TetO-Vegfc* mice (5.96 ± 1.404, n = 11) than *Osx-tTA* mice (9.231 ± 1.355, n = 9) mice. (**H,I**) Representative images of TRAP-stained femurs from *Osx-tTA* and *Osx-tTA;TetO-Vegfc* mice. (**J**) Graph showing the number of osteoclasts per mm of bone for *Osx-tTA* (1.18 ± 0.6818; n = 4) and *Osx-tTA;TetO-Vegfc* (6.84 ± 1.413; n = 4) mice. (**K**) Graph showing CTX-1 values for *Osx-tTA* (1.7 ± 2.045; n = 8) and *Osx-tTA;TetO-Vegfc* (53.3 ± 31.8; n = 7) mice. (***p<0.001, ****p<0.0001, unpaired student's T-test).

DOI: https://doi.org/10.7554/eLife.34323.008

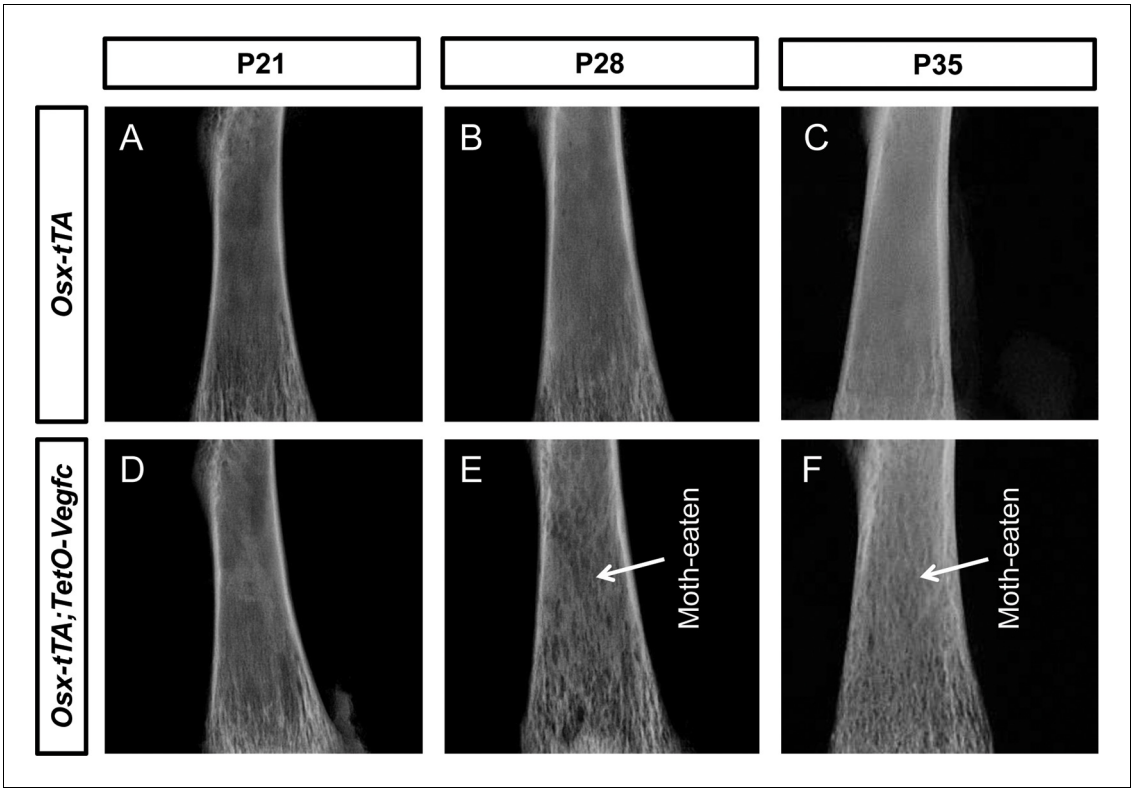

Figure 3—figure supplement 1. Bones from *Osx-tTA;TetO-Vegfc* mice have a moth-eaten appearance. Representative images of x-rayed femurs from *Osx-tTA* and *Osx-tTA;TetO-Vegfc* mice. (**A–C**) Femurs from P21, P28, and P35 *Osx-tTA* mice appear normal. (**D–E**) Femurs from P21 *Osx-tTA;TetO-Vegfc* mice appear normal, whereas femurs from P28 and P35 *Osx-tTA;TetO-Vegfc* mice have a moth-eaten appearance (arrows).

DOI: https://doi.org/10.7554/eLife.34323.009

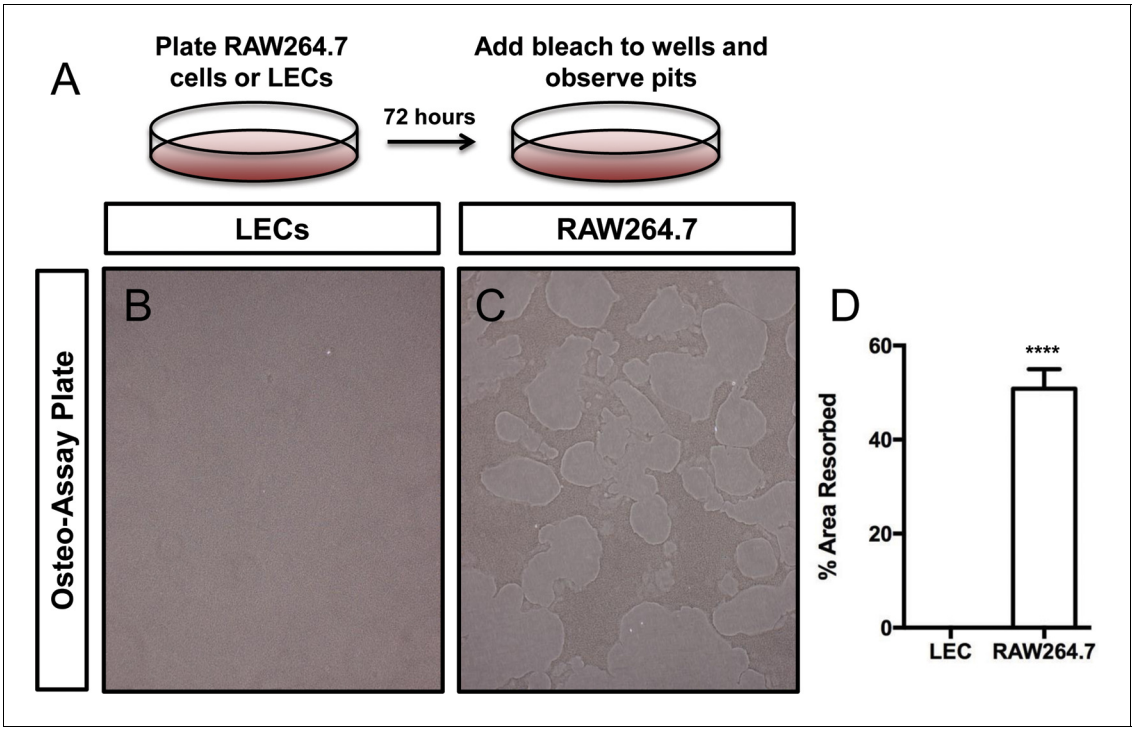

Figure 3—figure supplement 2. LECs do not degrade a calcium-phosphate matrix. (**A**) Schematic for experiment with the Osteo-Assay plate. (**B,C**) Representative images of wells containing lymphatic endothelial cells or RAW64.7 cells (osteoclasts). (**D**) Graph showing the percent area resorbed by lymphatic endothelial cells (0 ± 0.0; n = 3) and RAW264.7 cells (50.83 ± 4.131, n = 3). ****p<0.0001.

DOI: https://doi.org/10.7554/eLife.34323.010

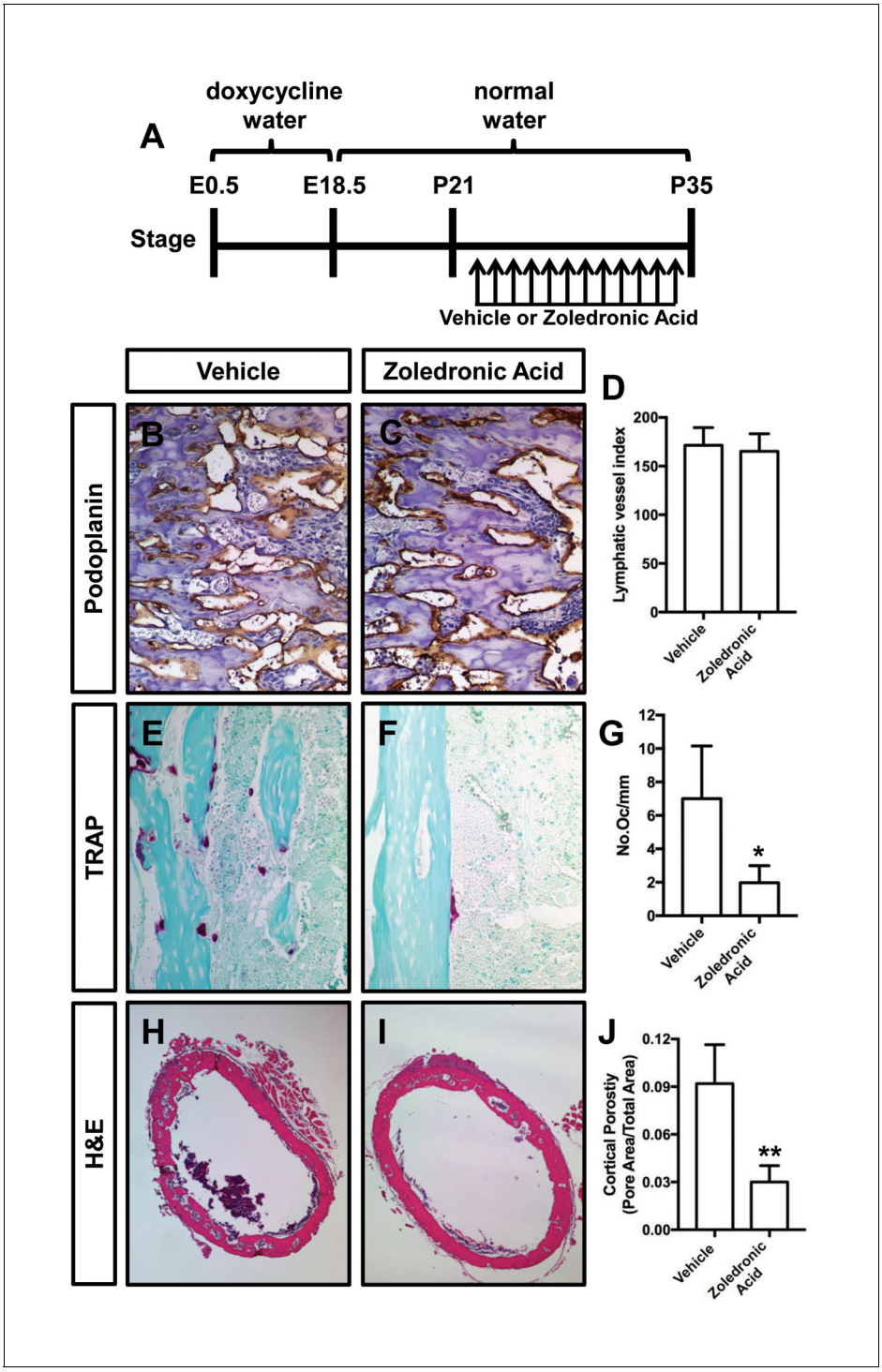

Figure 4. Zoledronic acid attenuates bone loss in *Osx-tTA;TetO-Vegfc* mice. (**A**) Schematic showing when mice received normal water and doxycycline water. *Osx-tTA;TetO-Vegfc* mice were treated (q.a.d.) with vehicle or zoledronic acid from P21 to P35. (**B,C**) Representative images of femurs stained with an anti-podoplanin antibody. (**D**) Graph showing lymphatic vessel index values for vehicle-treated (171.5 ± 18.18, n = 3) and zoledronic acid-treated (165.2 ± 18.04, n = 5) mice. (**E,F**) Representative images of TRAP stained femurs from vehicle-treated and zoledronic acid-treated mice. (**G**) Graph showing the number of osteoclasts per mm of bone for vehicle-treated (7.0 ± 3.15, n = 3) and zoledronic acid-treated (1.9 ± 1.9, n = 5) mice. (**H,I**) Representative images of H and E stained femurs from vehicle-treated and zoledronic acid-treated mice. (**J**) Graph showing cortical bone porosity of femurs for vehicle-treated (0.092 ± 0.0245, n = 3) and zoledronic acid-treated (0.030 ± 0.0103, n = 5) mice. (*p<0.05, **p<0.01, unpaired student's T-test).

DOI: https://doi.org/10.7554/eLife.34323.011

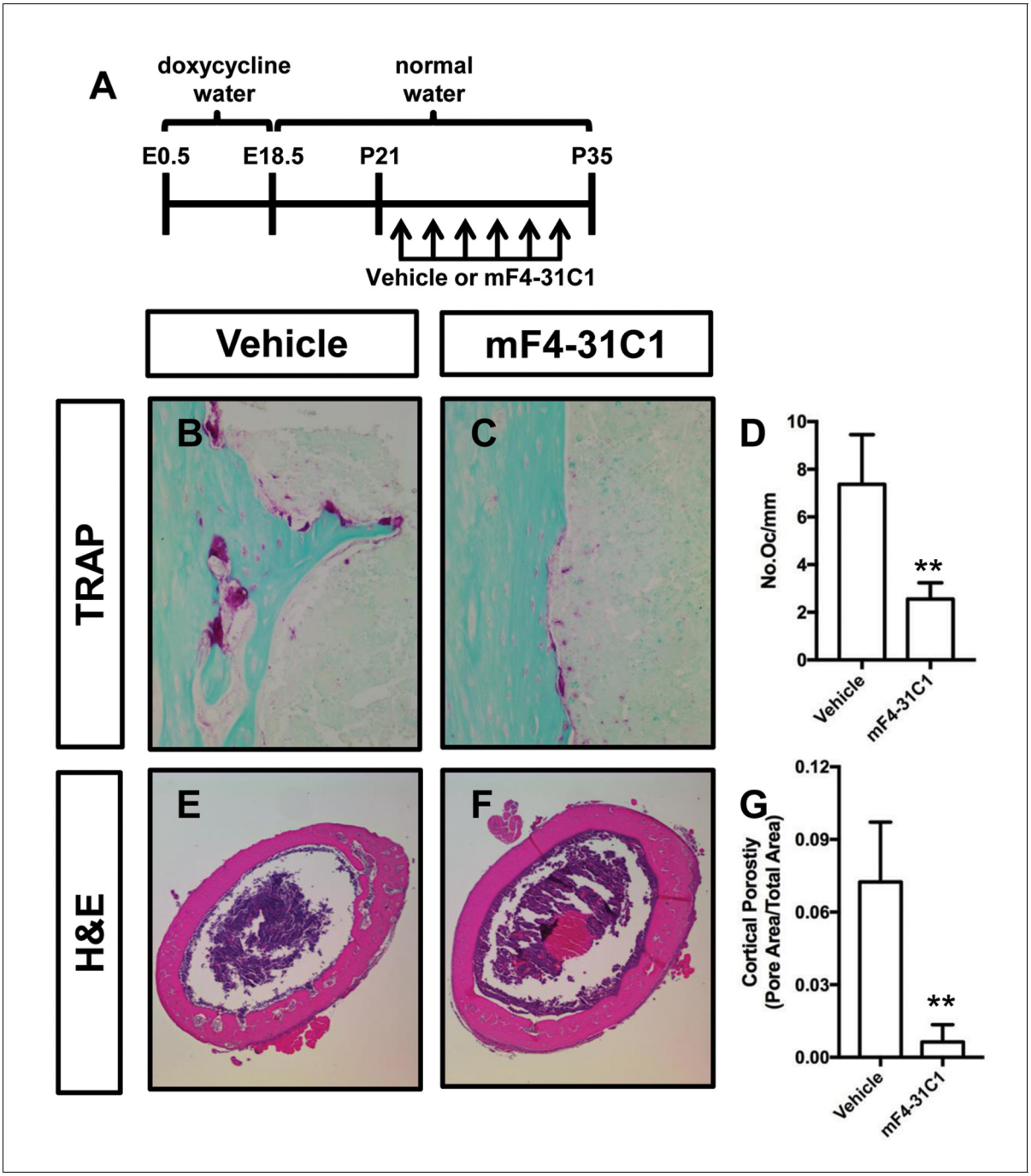

Figure 5. mF4-31C1 inhibits osteoclast formation and bone loss in *Osx-tTA;TetO-Vegfc* mice. (**A**) Schematic showing when mice received normal water and doxycycline water. *Osx-tTA;TetO-Vegfc* mice were treated (3x/week) with vehicle or mF4-31C1 (VEGFR3 function-blocking antibody) from P21 to P35. (**B,C**) Representative images of TRAP stained femurs from vehicle-treated and mF4-31C1-treated mice. (**D**) Graph showing the number of osteoclasts per mm of bone for vehicle-treated (7.37 ± 2.088, n = 5) and mF4-31C1-treated (2.552 ± 0.6893, n = 5) mice. (**E,F**) Representative images of H and E stained femurs from vehicle-treated and mF4-31C1-treated mice. (**G**) Graph showing cortical bone porosity of femurs for vehicle-treated (0.07244 ± 0.02468, n = 5) and mF4-31C1-treated (0.006375 ± 0.007087, n = 4) mice. (**p<0.01, unpaired student's T-test).

DOI: https://doi.org/10.7554/eLife.34323.012

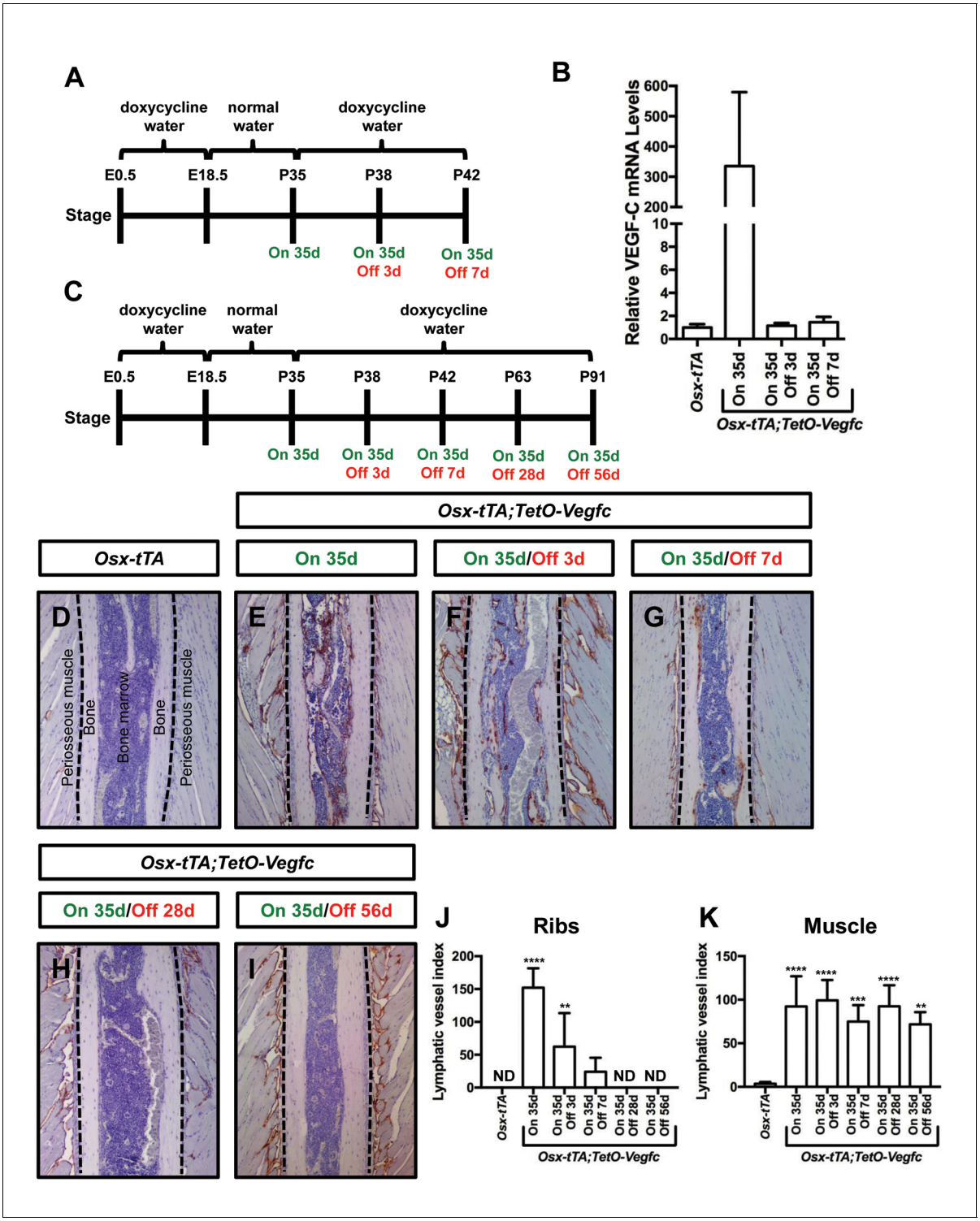

Figure 6. Bone lymphatics in *Osx-tTA;TetO-Vegfc* mice disappear following the withdrawal of VEGF-C. (**A**) Schematic showing when mice received normal water and doxycycline water. One cohort of *Osx-tTA;TetO-Vegfc* mice received normal water from E18.5 to P35 (On 35d). A second cohort of *Osx-tTA;TetO-Vegfc* mice received normal water from E18.5 to P35 and then doxycycline water from P35 to P38 (On 35d/Off 3d). A third cohort of *Osx-tTA;TetO-Vegfc* mice received normal water from E18.5 to P35 and then doxycycline water from P35 to P42 (On 35d/Off 7d). (**B**) Graph showing the relative VEGF-C mRNA levels in tibias from mice. (**C**) Schematic showing when mice received normal water and doxycycline water. *Osx-tTA;TetO-Vegfc* mice received normal water from E18.5 to P35 (On 35d) or normal water from E18.5 to P35 and then doxycycline water for 3 (On 35d/Off 3d), 7 (On 35d/Off 7d), 28 (On 35d/Off 28d), or 56 days (On 35d/Off 56d). (**D–I**) Representative images of ribs stained with an anti-podoplanin antibody. The dashed

Figure 6 continued on next page

Figure 6 continued

lines separate the bone from the periosseous muscle. (**J**) Graph showing lymphatic vessel index values for ribs in *Osx-tTA* mice (0 ± 0.0; n = 5), *Osx-tTA; TetO-Vegfc* mice that received normal water for 35 days (152.5 ± 29.56; n = 5), and *Osx-tTA;TetO-Vegfc* mice that received normal water for 35 days and then doxycycline water for 3 (62.25 ± 51.7; n = 4), 7 (24.08 ± 21.26; n = 4), 28 (0 ± 0.0; n = 5) or 56 (0 ± 0.0; n = 3) days. (**K**) Graph showing lymphatic vessel index values for periosseous muscle in *Osx-tTA* mice (3.61 ± 1.974; n = 5), *Osx-tTA;TetO-Vegfc* mice that received normal water for 35 days (92.45 ± 34.63; n = 5), and *Osx-tTA;TetO-Vegfc* mice that received normal water for 35 days and then doxycycline water for 3 (99.29 ± 23.37; n = 4), 7 (74.84 ± 18.98; n = 4), 28 (92.67 ± 24.2; n = 5) or 56 (72.17 ± 14.05; n = 3) days. (**p<0.01, ***p<0.001, ****p<0.0001, ANOVA followed by Dunnett's multiple comparisons test. Values were tested against values for *Osx-tTA* mice). ND = Not Detected.

DOI: https://doi.org/10.7554/eLife.34323.013

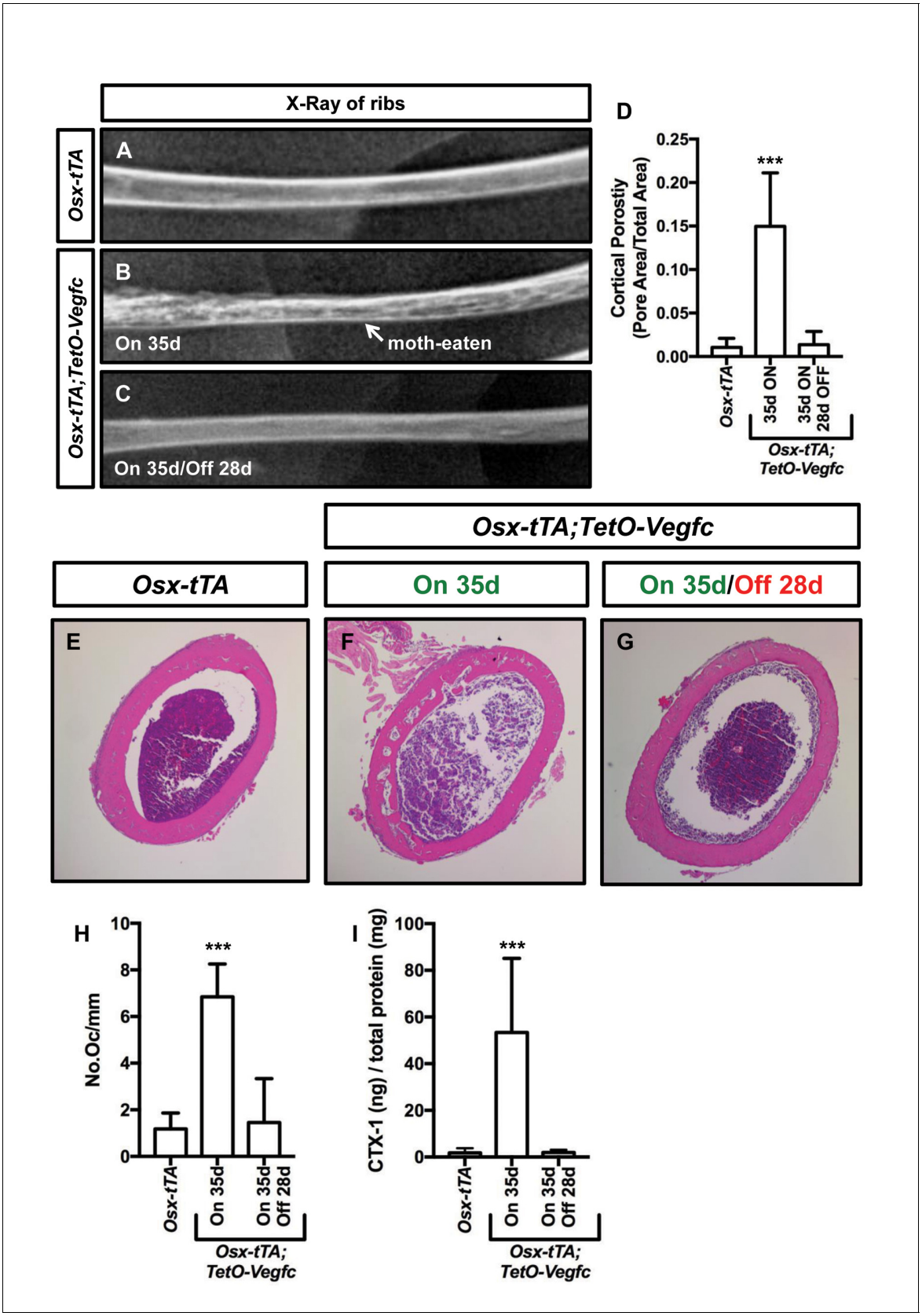

Figure 7. The bone phenotype of *Osx-tTA;TetO-Vegfc* mice is reversible. (**A–C**) Representative x-ray images of femurs from *Osx-tTA* mice, *Osx-tTA; TetO-Vegfc* mice that received normal water from E18.5 to P35 (On 35d), and *Osx-tTA;TetO-Vegfc* mice that received normal water from E18.5 to P35

Figure 7 continued on next page

Figure 7 continued

and then doxycycline water from P35 to P63 (On 35d/Off 28d). *Osx-tTA;TetO-Vegfc* femurs switched from a moth-eaten appearance to a normal appearance following exposure to doxycycline. (**D**) Graph showing cortical bone porosity values for femurs from *Osx-tTA* mice (0.011 ± 0.0103; n = 4), *Osx-tTA;TetO-Vegfc* mice that received normal water from E18.5 to P35 (0.149 ± 0.0615; n = 7), and *Osx-tTA;TetO-Vegfc* mice that received normal water from E18.5 to P35 and then doxycycline water from P35 to P63 (0.014 ± 0.0152; n = 5). (**E–G**) Representative images of H and E stained femurs. The femur from the *Osx-tTA;TetO-Vegfc* mouse that received normal water from E18.5 to P35 is filled with pores. (**H**) Graph showing the number of osteoclasts per mm of bone for *Osx-tTA* mice (1.18. ±0.6818; n = 4), *Osx-tTA;TetO-Vegfc* mice that received normal water from E18.5 to P35 (6.84 ± 1.41; n = 4), and *Osx-tTA;TetO-Vegfc* mice that received normal water from E18.5 to P35 and then doxycycline water from P35 to P63 (1.45 ± 1.88; n = 4). (**I**) Graph showing CTX-1 values for *Osx-tTA* mice (1.7 ± 2.045; n = 8), *Osx-tTA;TetO-Vegfc* mice that received normal water from E18.5 to P35 (53.3 ± 31.8; n = 7), and *Osx-tTA;TetO-Vegfc* mice that received normal water from E18.5 to P35 and then doxycycline water from P35 to P63 (1.9 ± 1.19; n = 4). (***$p<0.001$, ANOVA followed by Dunnett's multiple comparisons test. Values were tested against values for *Osx-tTA* mice.).

DOI: https://doi.org/10.7554/eLife.34323.014

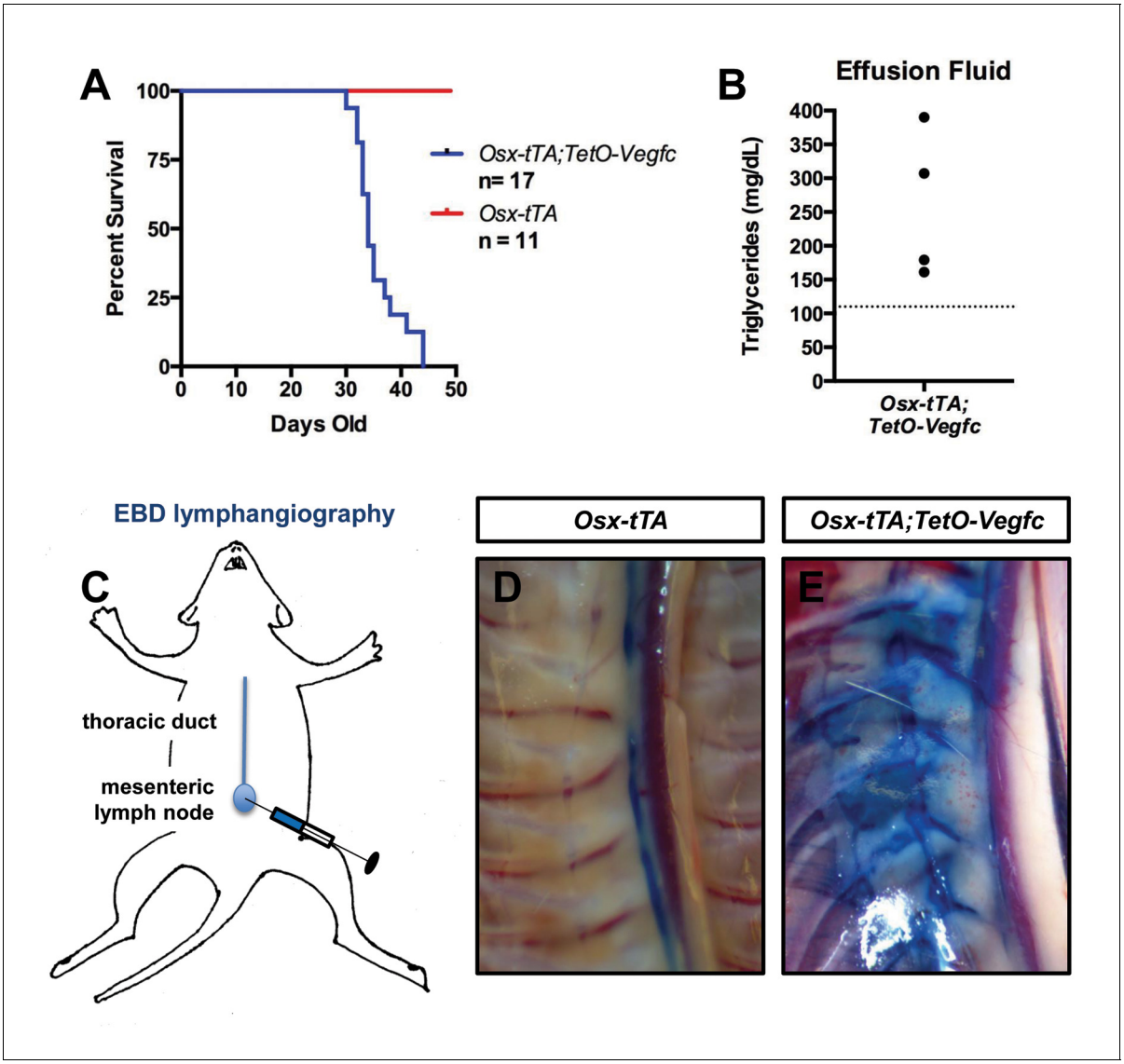

Figure 8. *Osx-tTA;TetO-Vegfc* mice develop chylothorax. (**A**) Survival curve for *Osx-tTA* and *Osx-tTA;TetO-Vegfc* mice ($p<0.0001$ Log-rank (Mantel-Cox) test). (**B**) Graph showing triglyceride levels in effusion fluid collected from *Osx-tTA;TetO-Vegfc* mice (n = 4). The dashed line marks 110 mg/dl. (**C**) Overview of the Evans blue dye (EBD) lymphangiography method. EBD injected into the mesenteric lymph node is transported to the thoracic duct. (**D**) EBD is confined to the thoracic duct in *Osx-tTA* mice (n = 4). (**E**) In *Osx-tTA;TetO-Vegfc* mice, EBD spills from the thoracic duct into periosseous lymphatics in muscle (n = 4).

DOI: https://doi.org/10.7554/eLife.34323.015